



OTC-29916-MS

Prediction of Wettability Alteration Using the Artificial Neural Networks in the Salinity Control of Water Injection in Carbonate Reservoirs

Leonardo Fonseca Reginato, Cleyton Carvalho Carneiro, Rafael Santos Gioria, and Marcio Sampaio Pinto,
Universidade de São Paulo

Copyright 2019, Offshore Technology Conference

This paper was prepared for presentation at the Offshore Technology Conference Brasil held in Rio de Janeiro, Brazil, 29–31 October 2019.

This paper was selected for presentation by an OTC program committee following review of information contained in an abstract submitted by the author(s). Contents of the paper have not been reviewed by the Offshore Technology Conference and are subject to correction by the author(s). The material does not necessarily reflect any position of the Offshore Technology Conference, its officers, or members. Electronic reproduction, distribution, or storage of any part of this paper without the written consent of the Offshore Technology Conference is prohibited. Permission to reproduce in print is restricted to an abstract of not more than 300 words; illustrations may not be copied. The abstract must contain conspicuous acknowledgment of OTC copyright.

Abstract

Artificial Neural Networks (ANN) applications have grown exponentially in all areas of science and technology. The advantages are its versatility, speed and ability to aggregate information, perform predictions of a given set of data. These attributes attract the petroleum industry, which often depends on laboratory analysis or numerical simulation to estimate various reservoir behaviors. This research, aims to predict the relative permeability curves with wettability alteration effect, given a concentration of the ionic composition in water injection. For this, machine learning methods were applied. An analytical algorithm was developed that incorporated the effect of wettability alteration, generating the database for the training process. Two different networks were applied: (i) Self-Organizing Maps - SOM and (ii) Neural Net Fitting – NNF. The forecast data of the networks are compared with calculated for analytical results. This ANN performs a good forecast of data tested (NNF with R-squared results around 90%). The analyses confirm effects on relative permeability of oil and water with salt control, indicating wettability alteration (WA). These tests were able to confirm that the applied methodology is capable to predict, using ANN, results of several laboratory tests.

Introduction

Currently, innovative reservoir production strategies are presented to improve techniques already known by the oil companies. One of them is the Low Salinity Water Injection (LSWI), where the secondary recovery method (common water injection) is used, but with the care of controlling the ions concentration to reduce residual oil saturation (Sor).

In Offshore exploration (the main scenario of Brazilian oil production), easy accessibility and preparation of the sea water to injection in the reservoir makes the LSWI a good tertiary recovery method to implement. To Dang et al. (2013a), the EOR method by salinity control shows advantages in terms of chemical costs, environmental impact, and field process implementation with compare to conventional chemical flooding.

According to Rezaeidoust et al. (2009), the injection of water as a secondary recovery method was applied for a long time. Recently, many studies focused on the ionic composition of this injection, pointed a tendency

to change the properties of wettability during the water flow in the reservoir. Thus, with the ideal ionic composition of this “smart water”, it would be possible to carry out a tertiary recovery process.

The hypothesis is based on injection water calibrated by salinity that provides a polar interaction between the potential ions (SO_4^{2-} , Mg^{2+} and Ca^{2+}) and the surface of rock, changing the oil-wet system due to influence by aqueous ions with the rock be stronger than hydrocarbon compounds. Wettability alteration (WA) procedure is a key parameter for improvement in oil production by this injection method (Webb et al., 2004; Seethepalli et al., 2004; Hirasaki et al., 2004; Fathi et al., 2011; Saikia et al., 2018).

Dang et al., (2013b) evaluate the study in the last two decades about salinity composition main effects in the reservoir conditions. These authors include the fines migration, multi-component ionic exchange (MIE), pH effect, electrical double layer effect, and the wettability alteration present in smart water injection.

The way to evaluate these effects is realizing the laboratory tests of these physicochemical process. So, many works applied the method of smart water injection on a laboratory scale. Through core-flooding tests, it is possible to evaluate with different dilutions of seawater the effects in relative permeability curves, contact angle, interfacial tension and other parameters with determined ionic concentration (Yousef et al., 2011; Ghosh et al., 2016; Bidhendi et al., 2018; Xiao et al., 2018). Although coreflooding tests produce a lot of information regarding the specific rock-fluid system, this knowledge is a singular behavior of each scenario.

To promote a general methodology for reservoir simulation studies, in the present work one proposes to apply the artificial neural networks method to be able to replicate these WA effects with injection of smart water in different carbonate reservoir scenarios. Testing the efficiency of two networks types to forecasting the permeability curves with salinity control and the different results between these networks tested. Also, evaluating the relation of the main parameters to calculate the permeability curves for each artificial neural network method.

Methodology

In order to overcome these problems, it was created an algorithm uses a correlation with salinity and residual oil saturation to represent a phenomenon of wettability alteration in the reservoir simulation model. This algorithm was developed to incorporates the WA process, expressed through the alteration of the relative permeability curves (K_r) of oil (K_{ro}) and water (K_{rw}). This method uses as input the initial permeability curves of a numerical reservoir model and salinity variation of the water injection, where the algorithm recalculates these K_r curves with a determined salinity. Thus, we used 13 synthetic models of simulation reservoirs to obtain data for ANN training and a more complex model with robust data, evaluating the accuracy of prediction of trained networks.

The input data (K_r curves, water saturation - S_w , Porosity - Por and absolute permeability - K_{abs}) and the output of low relative permeability curve (oil: K_{ro_LS} and water: K_{rw_LS}) calculated with the analytical algorithm, was imputed in Siro-SOM® software. The training was performed through selforganizing maps, which correlates the inputs and outputs of the model, making the network estimate the data values that were excluded in the training process (characterizing an unsupervised training).

The same database used for training with SOM's is also applied to a backpropagation-type ANN through Neural Net Fitting - NNF (supervised training). The objective of these training with two types of ANN is to compare the accuracy of these results with values obtained from the analytical model, may show a future substitution of laboratory tests of relative permeability by artificial neural networks. Also, SOM heat plots were evaluated and a contribution analysis of fitting network, to improve understanding of these input variables for networks.

Analytical Model

The algorithm used the initial configuration of relative permeability curves and calibrated a new curve based on the salinity of water injection. To add a good representation in the algorithm by WA effect in carbonate, the equations of two different authors were used. The first one corresponds to the equation developed by Brooks and Corey (1964) and the second one is the equations of Honarpour et al. (1986).

The difference between these two methods is due to the fact that the Brooks-Corey equations are generalized with respect to the type of formation, their wettability and the smoothing parameter of the permeability curves (Corey exponent, no and nw) that does not have an established standard in the literature, being commonly obtained through laboratory data fitting. In this work, one has assumed the Corey exponent equals 2. The equation proposed by Honarpour et al., (1986) presents differences according to the lithological type (carbonate and sandstone) and their wettability (ranging from wet to water and intermediate wet). Thus, this second method obtains results better adjusted to the characteristics of interest of this work, which considered only carbonate with intermediate wettability.

Brooks-Corey

$$k_{ro} = k_{rocw} \left(\frac{1 - S_w - S_{or}}{1 - S_{cw} - S_{or}} \right)^{no} \quad (1)$$

$$k_{rw} = k_{rwor} \left(\frac{S_w - S_{cw}}{1 - S_{cw} - S_{or}} \right)^{nw} \quad (2)$$

Equation (1) of oil relative permeability by Corey and Equation (2) of water relative permeability by Corey.

Honarpour et al

$$k_{ro} = 1,2614 \left(\frac{S_o - S_{or}}{1 - S_{or}} \right) \left(\frac{S_w - S_{cw}}{1 - S_{cw} - S_{or}} \right)^2 \quad (3)$$

$$k_{rw} = 0.29986 \left(\frac{S_w - S_{cw}}{1 - S_{cw}} \right) - 0,32797 \left(\frac{S_w - S_{or}}{1 - S_{cw} - S_{or}} \right)^2 (S_w - S_{cw}) + 0,413259 \left(\frac{S_w - S_{cw}}{1 - S_{cw} - S_{or}} \right)^4 \quad (4)$$

Equation (3)) of oil relative permeability for carbonate with intermediate wettability by Honarpour and Equation (4) of water relative permeability for carbonate with intermediate wettability by Honarpour.

Salinity Correlation

The equation of Brooks and Corey (1964) and Honarpour et al., (1986) are not directly related to salinity concentration in the water system. According to Dang et al. (2013b), the possibility of reservoir simulation using numerical integration with the effects of LSWI flooding accurately is still limited. Knowing this difficulty, Jerauld et al. (2006) developed a simple correlation to incorporate the salinity and the oil adsorbed on the surface of the rock. The authors observed the impact of salinity effect on the residual oil saturation of core samples. The results showed that the effect of salinity is not linear, as shown in Figure 1. They highlighted that, at a certain level of salinity, the effect in S_{or} is very low or insignificant, so they created an empirical dependence based on coreflooding results.

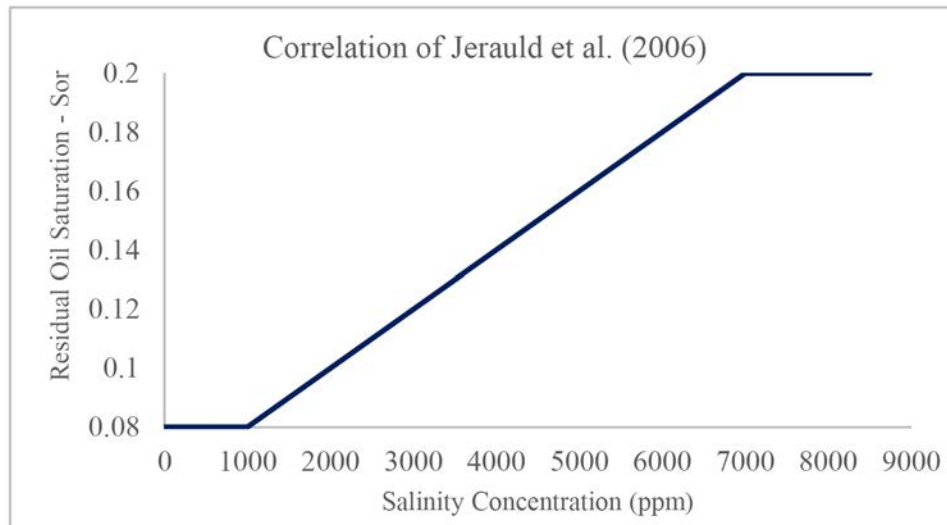


Figure 1—Correlation of Salt Concentration vs Residual Oil Saturation, adapted to Jerauld et al. (2006).

Database Generation

The database generation was a straightforward process: using the presented equations, one inputs different salinity concentrations and calculates the relative permeability with low salinity. The user needs to input the variation of the salt concentration ($\Delta salt$), with this variation, the algorithm calculates the new permeability curves with the initial salinity (1000 ppm) and the others data points by stepping the $\Delta salt$, until the final concentration (7000 ppm).

For this algorithm, the input parameters are listed below:

- Relative Permeability of Water - K_{rw} ;
- Relative Permeability of Oil - K_{ro} ;
- Water Saturation - S_w ;
- Mean Porosity - P_{or} ;
- Absolute Permeability - K_{abs} ;
- Variation of salt concentration - $\Delta salt$.

The WA algorithm calculates a series of K_{r_LS} curves, with different salt concentrations. Finally, the outputs of the database are grouped into:

- Relative Permeability of Water (Honarpour) - H_K_{rwLS} ;
- Relative Permeability of Oil (Honarpour) - H_K_{roLS} ;
- Relative Permeability of Water (Corey) - C_K_{rwLS} ;
- Relative Permeability of Oil (Corey) - C_K_{roLS} ;
- Mean of results of Relative Permeability of Water - M_K_{rwLS} ;
- Mean of results of Relative Permeability of Oil - M_K_{roLS} ;

The data are shaped into a matrix, resulting in an organized table for the training of the networks afterward. An average of the results of the relative permeability curves with the two methods (Corey and

Honarpour) is used obtained, seeking to minimize the error associated with every two methods of relative permeability estimation.

Artificial Neural Networks

Because the training process is different between the networks (unsupervised and supervised), it is necessary to organize the original database for each neural network used. As previously mentioned, two different ANNs are used, the first one is the SOM method, and the second is a NFF, both applied to predict WA behavior. Because the training process is different between the two networks (unsupervised and supervised), it is necessary to organize the original database for each neural network used, resulting in two new databases organization: Training database - SOM and Training database - Fitting. A part of the data is separated for the step of evaluation learning ability and generalization capacity of the networks. The workflow shown in Figure 2 illustrates the steps developed in this work:

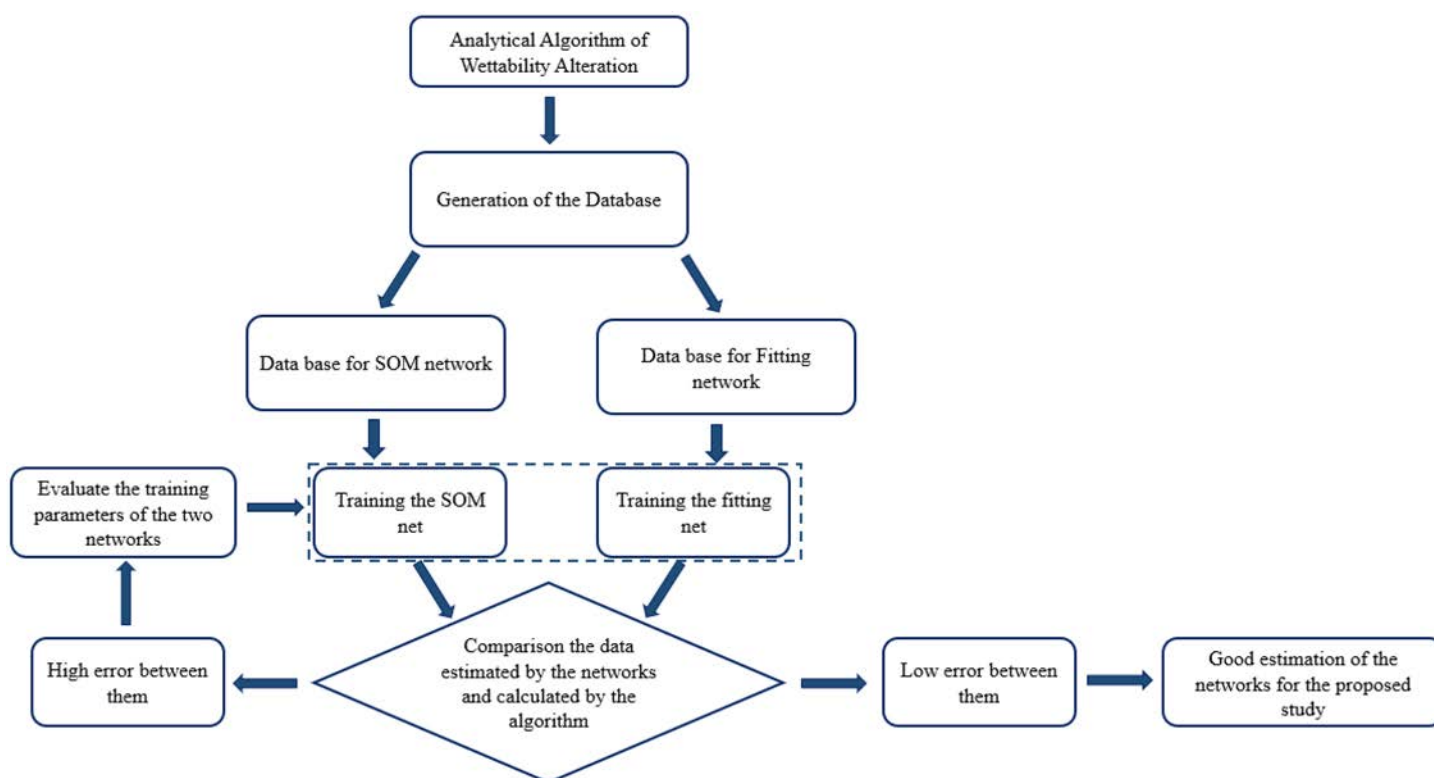


Figure 2—Workflow developed using two different ANNs.

Self-Organizing Maps

Self-Organizing Maps are considered a tool for analysis, visualization and interpretation of the data an n-dimensional space, using the similarity vector measurements (Fraser and Dickson, 2007). Knowing these advantages that SOM provides, this network is used to obtain the prediction of Kr curves with low salinity injection, integrating with the information on this set of variables, which initially do not present a direct correlation.

Part of permeability data is omitted to be forecast by the SOM network, realizing a comparison between the analytical and predicted results. Since the network follows an unsupervised training, where the network organizes the input data by similarity in the topological map, one does not need to provide a priori output information in the training process, as shown in Figure 3 below:

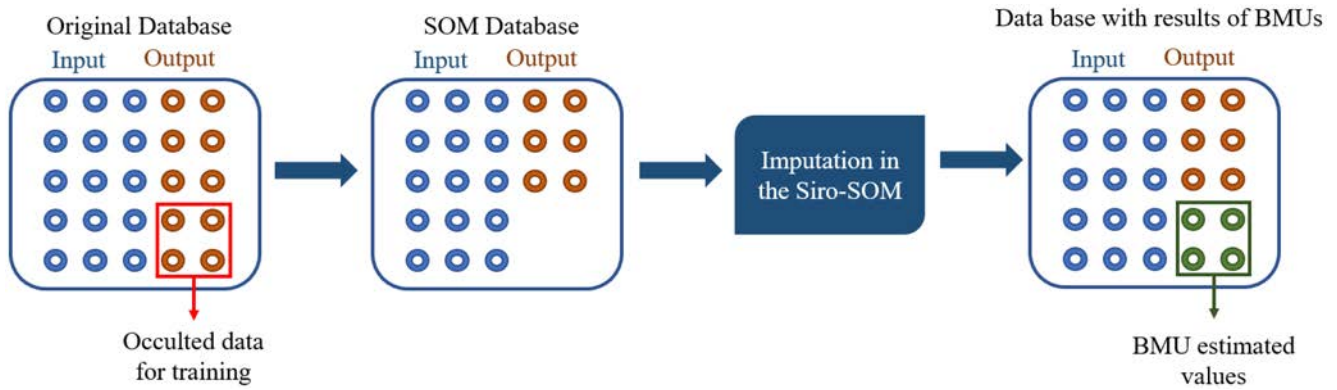


Figure 3—Illustration of data exclusion for unsupervised network.

Like all neural networks training process, some operational parameters should be assigned to develop the training and the analysis of results. Therefore, the evaluation of SOM-type network relied on two different sizes networks, called: Analysis-1 (network 26×26 neurons) and Analysis-2 (network 40×40 neurons). The calculation of size for Analysis-1 is performed through Equation 5 proposed by Vesanto et al. (1999):

$$N^{\circ} \text{ Neurons} = (5 * \sqrt{N^{\circ} \text{ Samples}}) \quad (5)$$

The database for SOM had 18,241 samples: using Eq. 5, the size of neurons maps is 26×26 . The second size of the network was chosen using the $12 * N^{\circ} \text{ Samples}$, which was larger than the first size. This provides a comparison between the results with different sizes, enables to evaluate the impact on the map size in the predictions. Therefore, the 40×40 map size was chosen.

The topology of both SOM-network used was the toroidal shape, this format preserves the periodicity of the data in transformed space and avoids the edge errors; and the cells had hexagonal characteristics, i.e. six interactions with neighboring neurons.

Neural Net Fitting

The fitting network presents a known architecture, separated into three main layers: Input Layer; Hidden Layer and Output Layer. This type of network has the characteristic feedforward type, which according to Al-bulushi et al. (2012) are networks with a simpler structure, propagating the information (signal) in a single direction (from the input layer to the output layer).

In this work, the backpropagation (BP) Levenberg-Marquardt (Levenberg, 1944) algorithm was used, the BP algorithm updates each neuron weight by calculating its gradients. The error between the output data and forecasting data are propagated to previous layers, updating this weight to minimizing the error.

This supervised network needs all the inputs and outputs data in the training stage. This requires a different data organization from the original database differently from the SOM type network, generating the database of the fitting network as shown in Figure 4.



Figure 4—Illustration of data exclusion for supervised network.

Neural Net Fitting uses the cross-validation method during training, seeking the network generalization through the data set. Thus, it is necessary to define the ratios that divide the database into three parts: learning, validation, and testing. In the learning phase, a part of the database is used to perform the training and adjustment of neuronal weights. The validation step seeks to minimize a pre-established error metric, and when this error level is reached, the test step is performed and the training is finalized. This method aims to ensure that in each step there are not the same ones given, this helps in minimizing overfitting problems of networks in general. Therefore, the database was divided into 75% of the data for training, 15% for validation and 10% for the test.

Another data adjustment for training network was the normalization of salt concentrations for each sample. The SOM network performs the normalization of data automatically in its training process, but in the fitting-network is necessary to normalize the input data manually. The parameters of relative permeability and saturation respect a range of 0 to 1, but the salinity and absolute permeability required a normalization for the neural network to assign relevance to those values that are in a thousand steps.

Case Study

As previously mentioned, the relative permeability data of numerical simulation models are used in the algorithm. In order to provide a sufficient number of samples for the network's training, 13 templates provided by the reservoir simulation software were used. These templates are numerical models of synthetic reservoirs with various characteristics. The K_r properties were obtained from these 13 synthetic models of carbonate reservoirs and were used to realize the training step and a more robust model for evaluating the trained networks forecasting.

Cerena-I Model

A synthetic reservoir model based on the Brazilian Pre-salt Jupiter field was used to compare the network prediction. It contains more complex features than the models used in the network training, this proves that even the network training with simplified models can have a good prediction of WA behavior in a complex reservoir.

The characteristics of the Cerena-I reservoir model are: size $21 \times 21 \times 50$ blocks, with the simulation time of 30 years of production in an inverted five-spot system (4 producers and 1 injector).

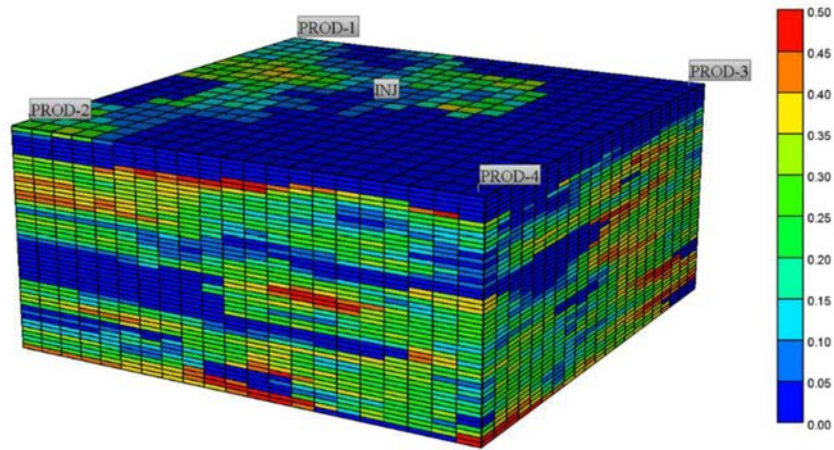


Figure 5—Cerena-I Simulation Model, showing the porosity distribution.

Results

SOM network

With the training of the SOMs networks, the prediction was analyzed using the BMUs of the Cerena-I data (excluded in the training phase) as imputation variables. Through the R-squared metric, it is possible to infer the accuracy of these estimates with the results calculated by the analytical algorithm. Thus, the correlation of data is presented in Figure 6:

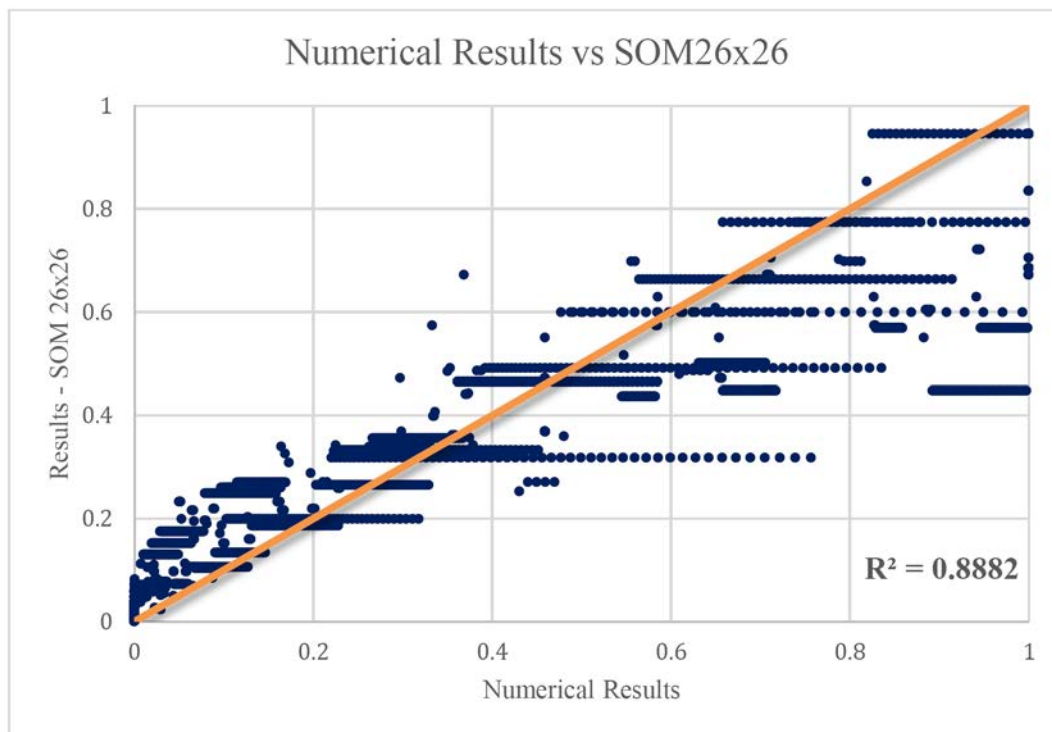


Figure 6—Correlation plot and R^2 between the numerical results and estimated by the SOM network (map 26×26).

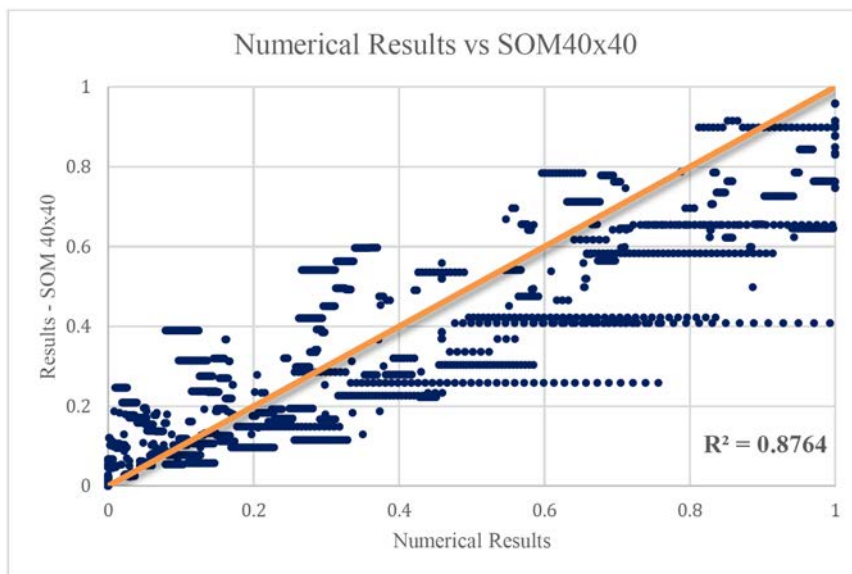


Figure 7—Correlation plot and R² between the numerical results and estimated by the SOM network (map 40x40).

The results obtained from the BMU's of the two SOM maps are satisfactory, with R² around 88%. The 26×26 network has a better R-squared value (approximately 0.12% better), a subtle difference. The orange line represents R² = 1, this reference line ensures to evaluate the dispersion of data, when the data set follow the orange line pattern, better is the network forecast. In these two networks, it is possible to see a large dispersion of results, although R-squared is high, the results still distant from the expected value. The pattern of horizontal distribution of these data (in blue) can be explained by the aggregation of similar data in a single neuron (BMU), that makes the group of real values has the same prediction value referent this neuron.

A random salinity was chosen to evaluate the Kr curves with this salt concentration. Thus, for all analyses, the results of 3700 ppm salt concentration were considered in this comparison. The objective is to quantify the difference between the relative permeability curves and to analyze if this neural network outputs useful results. In Figures 8 and 9, it is depicted the behavior of the curve generated by SOM compared to the curve calculated by the analytical method:

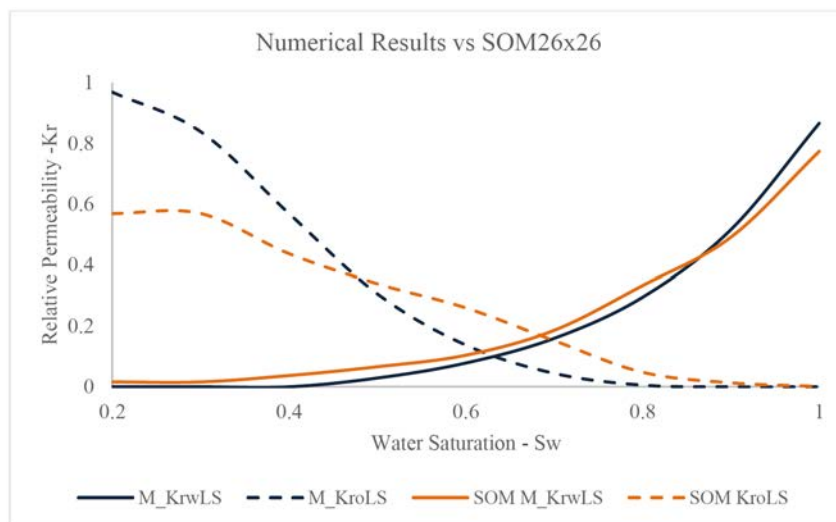


Figure 8—Relative permeability plot, comparing the mean of the analytical results versus the mean value of the SOM network (26×26 map).

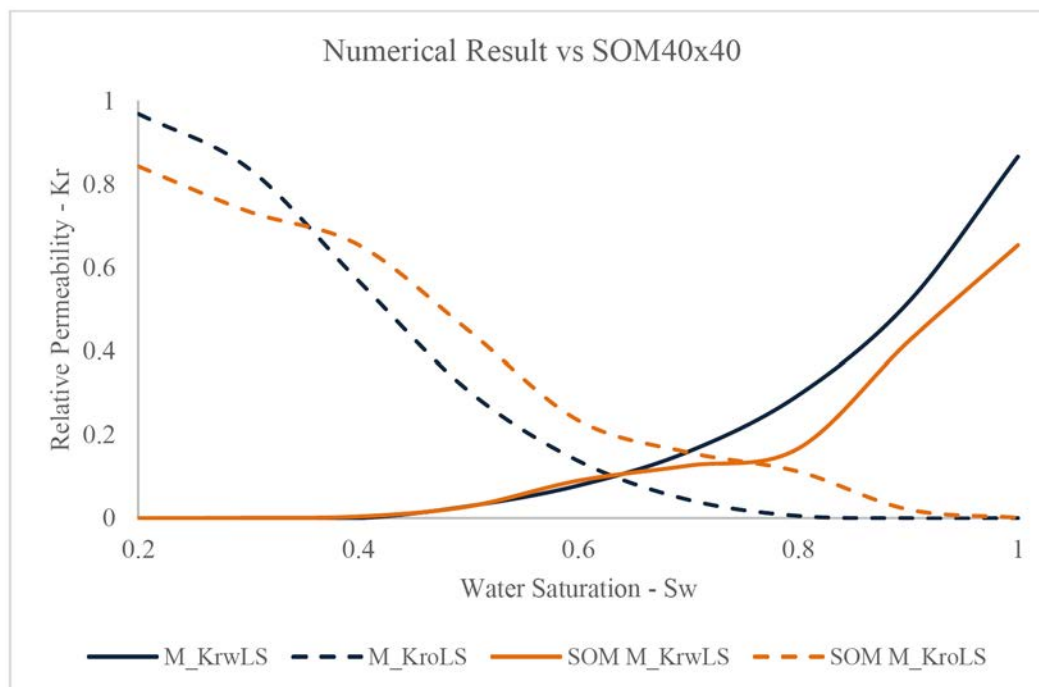


Figure 9—Relative permeability plot, comparing the mean of the analytical results versus the mean value of the SOM network (40x40 map).

Note that the 26×26 network (Fig. 8) is more accurate in the K_{rw} curve fitting (continuous line), being the only satisfactory fit between the SOM and numerical results. But, in general, SOM networks present poor adjustments with values calculated numerically. This analysis confirms an important characteristic of SOM type networks, whose goal is the data reduction, hence the BMUs follow this generalization to the predicted data and this feature may end up compromising the quality of the forecast of this data.

Another result that the SOM network provides is the component plots (CP), which visually represents data. Thus, it is possible to evaluate the pattern of these input variable values and infer the effect of a given variable on another. For instance, the pattern associated with residual oil saturation, porosity and absolute permeability of the models is discussed. The plots show that with medium-high porosity and high absolute permeability, the saturation of this residual oil is quite low (Figure 10).

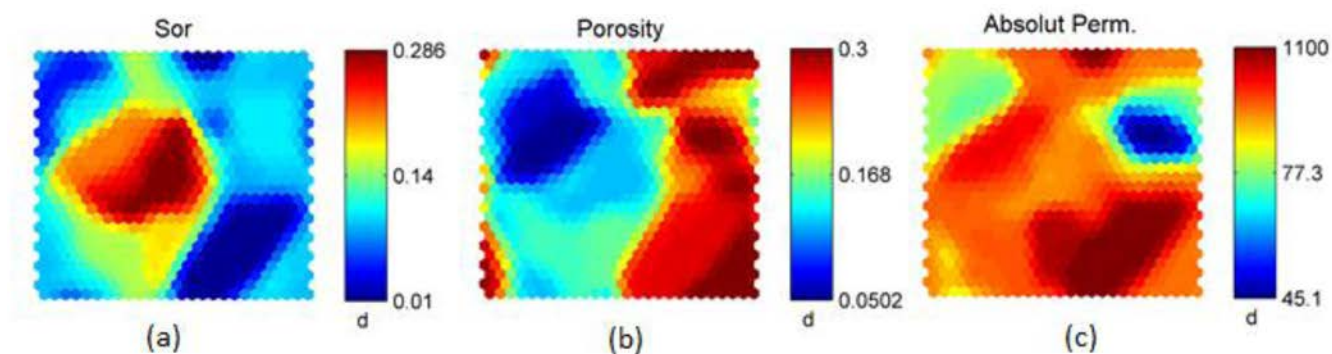


Figure 10—(a) Heat plot of Residual Oil Saturation by SOM26×26; (b) Heat plot of Porosity by SOM26×26; (c) Heat plot of Absolute Permeability by SOM26×26.

Another aspect observed in heat maps is that the high critical water saturation parameters (the point where the water begins to be mobile) are related to relative permeability curves with low values. In Figure 11, a

strong correlation between these rather high values of Scw with very low results from the initial point of oil permeability curve ($Krow$) and the end of the water permeability (Krw) curve may be noted.

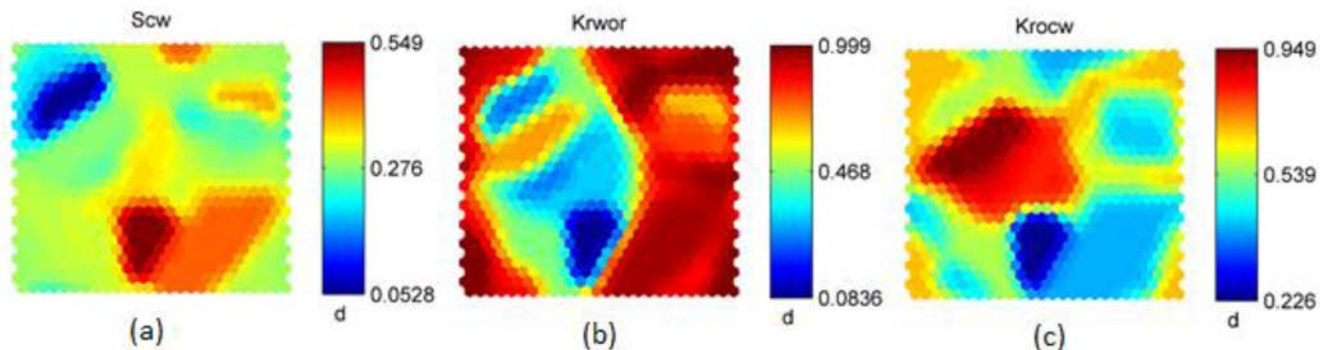


Figure 11—(a) Heat plot of Critical Water Saturation by SOM26x26; (b) Heat plot of Relative Permeability of Water with Residual Oil by SOM26x26; (c) Heat plot of Relative Permeability of Oil with Critical Water by SOM26x26.

The effects of salinity control can be seen by comparing the normal Kr plots and Kr_{LS} . In Figure 12, it is notable that relative permeability of oil with low salinity (Figure 12d) is related to a higher dispersion of high values compared to conventional injection. Thus, this salinity control obtained higher Kro in the models tested. This effect of salinity also occurred in the permeability of water, wherewith conventional injection (Figure 12a) it has a higher number of high values with a maximum of 0.997 and with the salinity control, the water permeabilities have experimented a reduction in their maximum value to 0.762 and a decrease in the number of samples that obtained these maximum value. Thus, the salinity control seems to have an effect of increasing the relative permeability of oil and reduction of water permeability values, indicating the effect of wettability alteration.

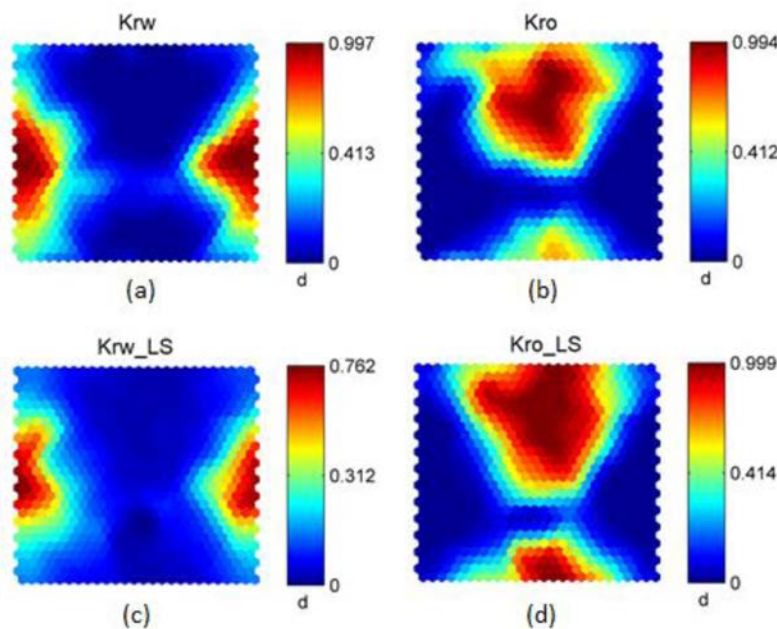


Figure 12—(a) Heat plot of Relative Permeability of Water by SOM26x26; (b) Heat plot of Relative Permeability of Oil by SOM26x26; (c) Heat plot of Relative Permeability of Water with Low Salinity by SOM26x26; (d) Heat plot of Relative Permeability of Oil with Low Salinity by SOM26x26.

All the analyzed figures were presented for the 26×26 network, which has shown a better prediction result based on the coefficient of determination. Nevertheless, the analysis based on the 40×40 network results in similar conclusions.

Fitting Network

Following the previous analyses, the performance of the fitting network results compared to the analytical results is discussed. Three networks with different dimensions in its hidden layer, chosen arbitrarily as 15, 17 and 26 neurons, were trained. The prediction results are shown in Figures 13, 14 and 15.

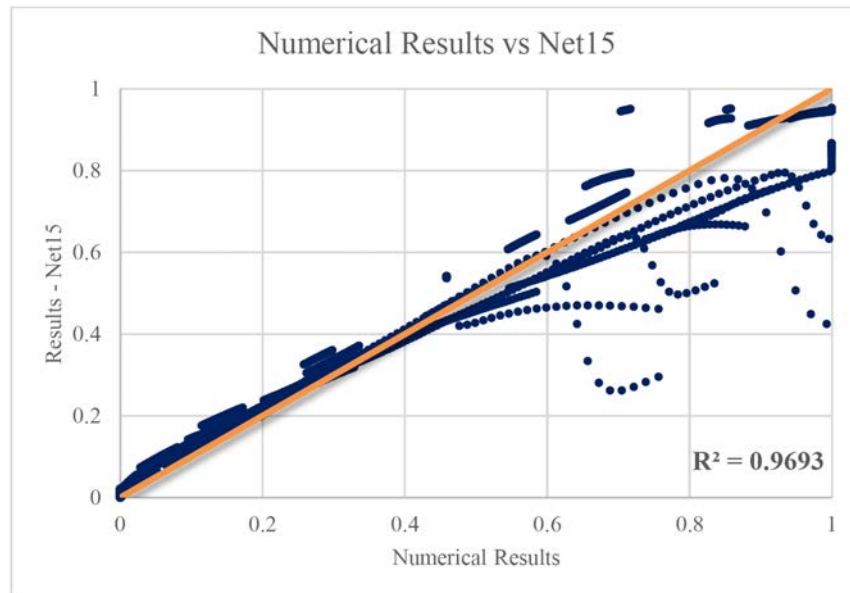


Figure 13—Correlation plot and R^2 between the numerical result and estimated by the fitting network (size net 15).

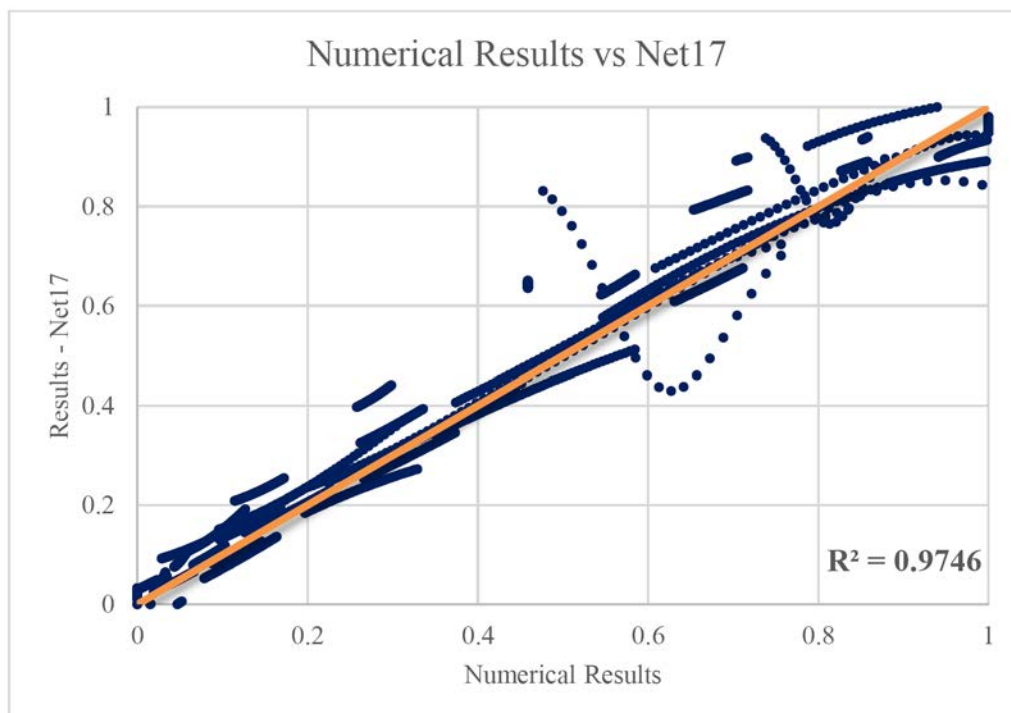


Figure 14—Correlation plot and R^2 between the numerical results and estimated by the fitting network (size net 17).

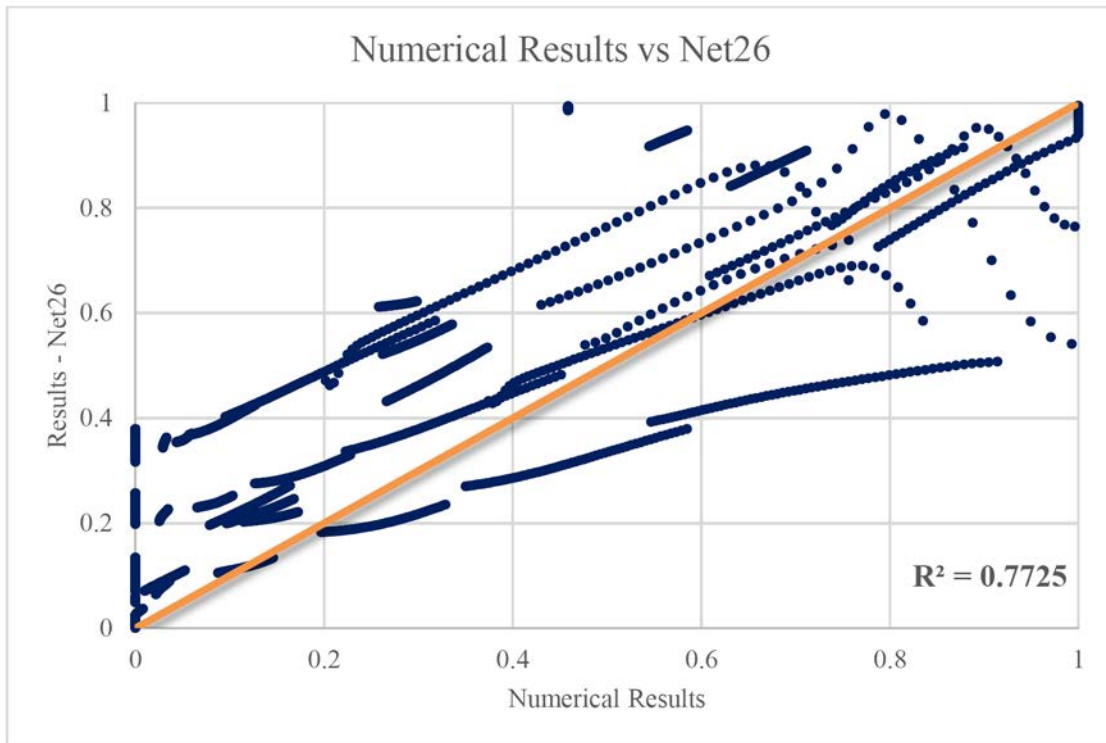


Figure 15—Correlation plot and R² between the numerical results and estimated by the fitting network (size net 26).

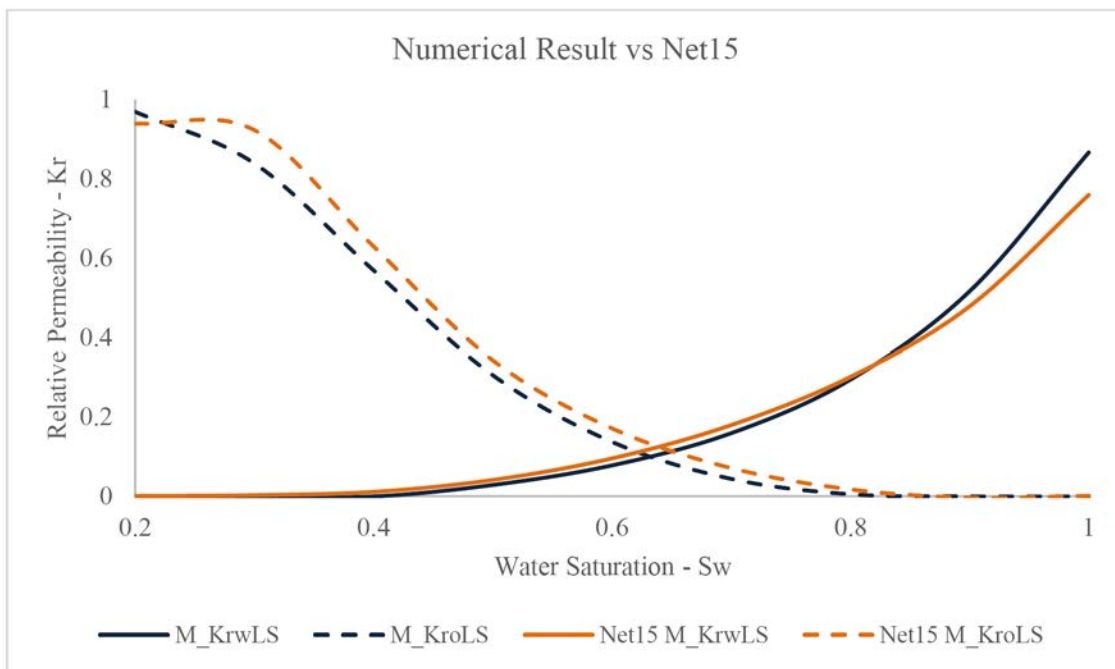


Figure 16—Relative permeability curves, compared with the mean of the numerical results versus the mean value of the fitting network (Net15).

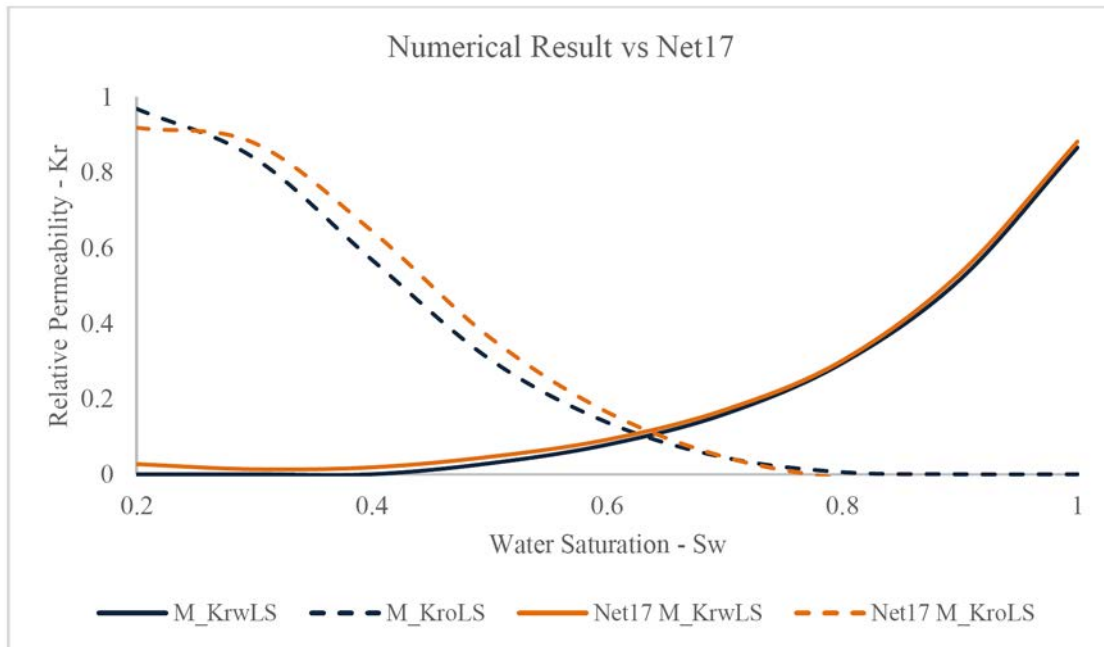


Figure 17—Relative permeability curves, compared with the mean of the numerical results versus the mean value of the fitting network (Net17).

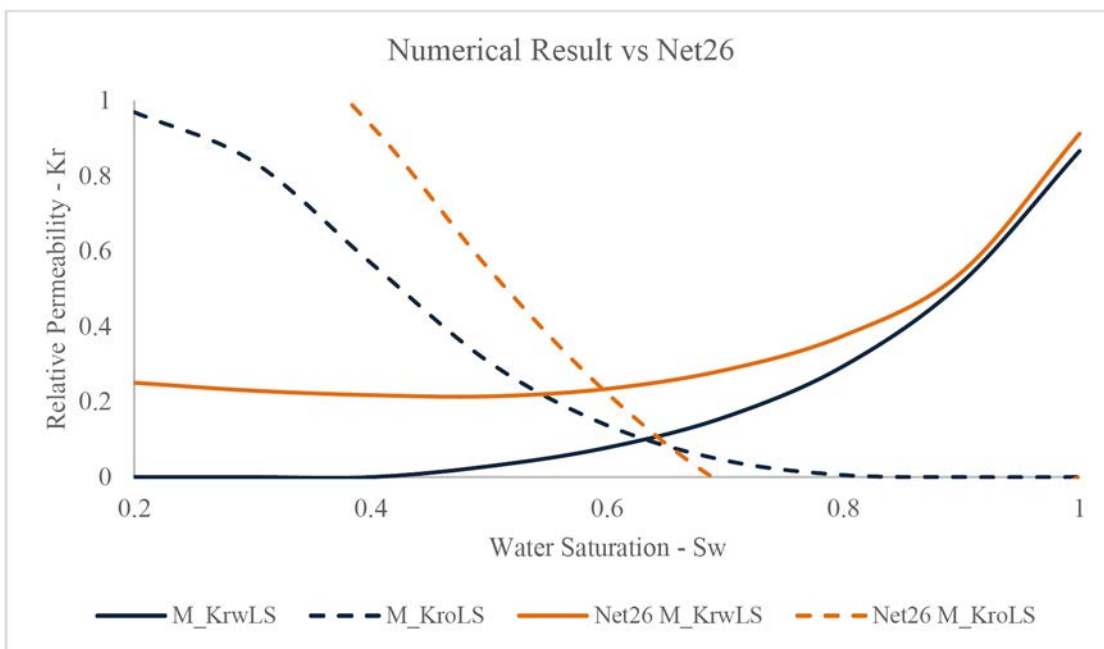


Figure 18—Relative permeability curves, compared with the mean of the numerical results versus the mean value of the fitting network (Net26).

It is possible to observe better estimates of “Net15” and “Net17” networks compared to the data obtained by the SOMs method, with the exception of “Net26” results, which is below results of all networks applied, around 11% loss of fit. This shows the sensitivity and importance of network size to obtain a good data fit. Considering the training method, input data and operational parameters of the three networks were the same, changing the size of neurons in the hidden layer equal to 26 neurons was the reason that poor performance in the fit. Jinchuan and Xinzhe (2008), developed an empirical analysis of the optimal number of hidden neurons, they suggest when the hidden neurons (units) are over-estimated, results in poor R^2 in the prediction phase, caused by overfitting network training. This effect occurs in the Net26 training shown above.

Using the reference value (orange line) is possible to see a good adjusted with the numerical results and the estimate of Net 15 and Net17. Another forecasting behavior is the worst fit in high values, the data between 0.5 to 1.0 indicate more difficult to predetermining by these nets.

Following the discussion of SOM results, the relative permeability curves of oil and water were plotted for the same concentration previously chosen (3700 ppm):

It is possible to compare the performance between the three network sizes (15, 17 and 26) and two networks of the SOM method. As their respective coefficients of determination (Figures 13 and 14) have already shown, Net15 and Net17 network prediction results fit well the results of the numerical algorithm, as expected by the coefficients of determination. The Net26 network has shown mismatched forecast results, which is also observed in its R^2 . Thus, Net17 has the best fit and R-squared, although it obtained Kr curves very similar to the results of Net15.

Defining the Net17 network with better forecast fitting, the last analysis was made for this network to obtain the contribution of each input variable to the neural network. According to the authors [Gevrey et al. \(2003\)](#), there are methods that aim to quantify the influence of input parameters on the network response. In this work, the so-called "Perturb" Method was used. In this method, a variation δ (noise) in each input variable is applied and one forecast at a time with data with noise $x_i = x_i + \delta$. By varying this δ in a probability distribution, it is possible to obtain the effects that the high and low noise magnitude may cause in the output of data, being able to classify these entries in order of importance.

Thus, a normal distribution was used to sample the noise applied in the data, with a standard deviation of 1.5 and mean 5. Finally, to define a sample number, we used a number of simulations with "X" cases (X noise values in each input parameter), of these cases, we selected "X/3" random samples, if the R-squared mean between noise prediction and normal prediction of "X/3" samples were equal to the R-squared mean of the "X" samples, then the sample number was good enough to represent the study. Thus, it was defined with 300 samples with noise, obtaining its R^2 average equal to 100 samples collected at random, calculate the contribution index by the mean of R-squared of all 300 samples less 1 ($Cidx = R^2 - 1$), since as greater the R-squared between the data with and without noise, smaller its relevance to the network estimative.

For Net17, water saturation has the greatest sensibility to the forecast of the outputs, the permeability of water and oil does not exceed 20% of the contribution of the results of this network. The absolute permeability is the least impacting to the network and the points of critical saturation of water and residual oil saturation also shows a significant contribution, and the salinity acts with the alteration of the parameter of residual saturation of oil. However, even though the salinity presents a low contribution to the result, the Sor's effect can be added to its contribution, causing the network to interpret the correlation between salinity and Sor through this contribution index.

An interesting observation of contribution index is the major parameters (water saturation - Sw, critical water saturation - Scw and residual oil saturation - Sor) elected by the network are present in the two numerical equations methods used in data construction. That's can indicate the process of learning of NNF can capture these main parameters for the numerical model.

Conclusion

In this work, analysis of uses of two well-established artificial neural networks was presented. The coefficient of determination was calculated between the numerical model and estimated by all the networks and it was chosen as a way of comparing the performance of the two networks for the prediction of the relative permeability curves with low salinity water injection. As previously mentioned, the fitting networks obtained much better results than two SOM method networks (their best result at Net17 with $R^2 = 0.9746$). It is important to note that Net26 fitting method presented a worse adjustment than two SOM's networks. This can be justified by the size of this network hidden layer, a super estimation of neurons that caused overfitting of this network, losing its characteristic of generalization to other data not included in the training set.

Therefore, feedforward networks such as the Neural Net Fitting - NNF used, have more accurate forecasting results and are better suited to predict this data. It is still necessary to obtain some results through laboratory analysis and using an analytical solution method to structure a database, applying posteriorly in the training of this NNF. However, the influence of network size on forecasting should be considered, testing different network sizes because the nature and quantity of the data are direct influencers in this estimation.

By computing the contribution index, it was possible to observe the correlation between the values of residual oil saturation with the salinity defined for water injection. Figure 19 shows that this correlation ends up having a greater contribution to the net result than the relative permeability curves without the LSWI.

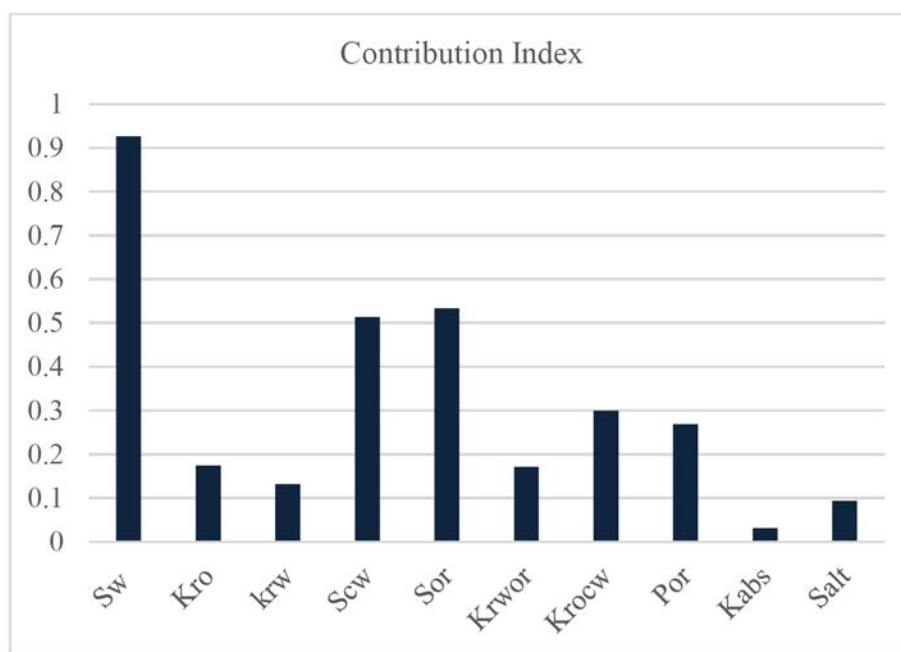


Figure 19—Contribution Index for the network Net17.

Through the heat plots results from SOM, it was possible to interpret some correlations that the NNF does not usually present. These plots illustrate the effect of salinity compared to the relative permeability of water and oil with and without low salinity water (Fig. 12), showing a decrease in water permeability curves with low water injection salinity and increase of the relative permeability of oil, present effect in the inversion of the wettability of the reservoir (for water wet).

Although the fitting networks are more indicated in the forecasting focus, this does not exclude the contributions of SOM networks. One may lose accuracy of fitting and may still obtain more information about the set of variables studied. With this network, it is possible to interpret of the importance of variables of the training set, to assist in the verification of hypotheses, or to show its influences in the network, adding value in the final analysis of the study.

Acknowledgments

The authors would like to thank LASG (Laboratory of Petroleum Reservoir Simulation and Management), InTRA (Integrated Technology for Rock and Fluid Analysis), Polytechnic School of the University of Sao Paulo, PETROBRAS S/A, Brazilian National Agency of Petroleum, Natural Gas and Biofuels (ANP) and FAPESP for supporting this work, and CMG®, MATLAB® and Siro-SOM® for software licenses.

References

- Al-Bulushi, N. I., P. R. King, M. J. Blunt, and M. Kraaijeveld, 2012, *Artificial neural networks workflow and its application in the petroleum industry: Neural Computing and Applications*, v. **21**, no. 3, p. 409–421, doi:[10.1007/s00521-010-0501-6](https://doi.org/10.1007/s00521-010-0501-6).
- Bidhendi, M. M., G. Garcia-Olvera, B. Morin, J. S. Oakey, and V. Alvarado, 2018, *Interfacial Viscoelasticity of Crude Oil/Brine: An Alternative Enhanced-Oil-Recovery Mechanism in Smart Waterflooding: SPE Journal*, v. **23**, no. 03, p. 0803–0818, doi:[10.2118/169127-pa](https://doi.org/10.2118/169127-pa).
- Brooks, R. H., and A. T. Corey, 1964, *Hydraulic properties of porous media: Fort Collins, Colorado, Colorado State U.*, 1–25 p.
- Dang, Cuong Thanh Quy, L. X. Nghiem, Z. J. Chen, and Q. P. Nguyen, 2013, Modeling Low Salinity Waterflooding: Ion Exchange, Geochemistry and Wettability Alteration: SPE Annual Technical Conference and Exhibition held in New Orleans, Louisiana, USA, no. 1995, doi:[10.2118/166447-ms](https://doi.org/10.2118/166447-ms).
- Dang, Cuong T. Q., L. X. Nghiem, Z. Chen, Q. P. Nguyen, and N. T. B. Nguyen, 2013, State-of-the Art Low Salinity Waterflooding for Enhanced Oil Recovery, in SPE Asia Pacific Oil & Gas Conference and Exhibition held in Jakarta, Indonesia: doi:[10.2118/165903-ms](https://doi.org/10.2118/165903-ms).
- Fathi, S. J., T. Austad, and S. Strand, 2011, *Water-based enhanced oil recovery (EOR) by “smart water”: Optimal ionic composition for EOR in carbonates: Energy and Fuels*, v. **25**, no. 11, p. 5173–5179, doi:[10.1021/ef201019k](https://doi.org/10.1021/ef201019k).
- Fraser, S. J., and B. L. Dickson, 2007, A New Method for Data Integration and Integrated Data Interpretation: Self-Organising Maps: Proceedings of Exploration 07: Fifth Decennial International Conference on Mineral Exploration, p. 907–910.
- Gevrey, M., I. Dimopoulos, and S. Lek, 2003, *Review and comparison of methods to study the contribution of variables in artificial neural network models: Ecological Modelling*, v. **160**, no. 3, p. 249–264, doi:[10.1016/S0304-3800\(02\)00257-0](https://doi.org/10.1016/S0304-3800(02)00257-0).
- Ghosh, B., L. Sun, and S. Osisanya, 2016, *Smart-Water EOR Made Smarter A Laboratory Development*: no. November, p. 14–16, doi:[10.2523/18988-ms](https://doi.org/10.2523/18988-ms).
- Hirasaki, G., D. L. Zhang, and U. Rice, 2004, *Surface Chemistry of Oil Recovery From Fractured, Oil- Wet, Carbonate Formations: Spe*, v. **88365**, p. 151–162.
- Honarpour, Mehdi, Koederitz, L., and A. H. Harvey, 1986, *Relative Permeability of Petroleum Reservoirs.pdf: Boca Raton, Florida, CRC Press*, 143 p., doi:[10.1201/9781351076326](https://doi.org/10.1201/9781351076326).
- Jerauld, G. R., C. Y. Lin, K. J. Webb, and J. C. Secombe, 2006, SPE 102239 Modeling Low-Salinity Waterflooding: SPE Annual Technical Conference, doi:[10.1002/app.30886](https://doi.org/10.1002/app.30886).
- Jinchuan, K., and L. Xinzhe, 2008, Empirical analysis of optimal hidden neurons in neural network modeling for stock prediction: Proceedings – 2008 Pacific-Asia Workshop on Computational Intelligence and Industrial Application, PACIIA 2008, v. **2**, p. 828–832, doi:[10.1109/PACIIA.2008.363](https://doi.org/10.1109/PACIIA.2008.363).
- Levenberg, K., 1944, *A Method for the Solution of Certain Non-Linear Problems in Least Squares: Quarterly of Applied Mathematics*, v. **1**, no. 278, p. 536–538, doi:[10.1090/qam/10666](https://doi.org/10.1090/qam/10666).
- Rezaeidoust, A., T. Puntervold, S. Strand, and T. Austad, 2009, *Smart water as wettability modifier in carbonate and sandstone: A discussion of similarities/differences in the chemical mechanisms: Energy and Fuels*, v. **23**, no. 9, p. 4479–4485, doi:[10.1021/ef900185q](https://doi.org/10.1021/ef900185q).
- Saikia, B. D., J. Mahadevan, and D. N. Rao, 2018, *Exploring mechanisms for wettability alteration in low- salinity waterfloods in carbonate rocks: Journal of Petroleum Science and Engineering*, v. **164**, no. December 2017, p. 595–602, doi:[10.1016/j.petrol.2017.12.056](https://doi.org/10.1016/j.petrol.2017.12.056).
- Seethepalli, A., B. Adibhatla, and K. K. Mohanty, 2004, *Physicochemical Interactions During Surfactant Flooding of Fractured Carbonate Reservoirs: SPE Journal*, v. **9**, no. 04, p. 411–418, doi:[10.2118/89423-pa](https://doi.org/10.2118/89423-pa).
- Vesanto, J., J. Himberg, E. Alhoniemi, and J. Parhankangas, 1999, Self-Organizing Map in Matlab: the SOM Toolbox: In Proceedings of the Matlab DSP Conference, p. 35–40.
- Webb, K. J., C. J. J. Black, H. Al-Ajeel, and S. Members, 2004, Low Salinity Oil Recovery-Log-Inject-Log, in Fourteenth Symposium on Improved Oil Recovery: p. 17–21, doi:[10.2118/89379-MS](https://doi.org/10.2118/89379-MS).
- Xiao, R., R. Gupta, R. C. Glotzbach, S. Sinha, and G. F. Teletzke, 2018, *Evaluation of low-salinity waterflooding in Middle East carbonate reservoirs using a novel, field-representative coreflood method: Journal of Petroleum Science and Engineering*, v. **163**, no. October 2017, p. 683–690, doi:[10.1016/j.petrol.2017.10.070](https://doi.org/10.1016/j.petrol.2017.10.070).
- Yousef, A. A., S. Al-Saleh, and M. S. Al-Jawfi, 2011, Smart WaterFlooding for Carbonate Reservoirs: Salinity and Role of Ions, in SPE Middle East Oil and Gas Show and Conference held in Manama, Bahrain: p. 1–11, doi:[10.2118/141082-ms](https://doi.org/10.2118/141082-ms).